

Structure, tectonic and petrology of mid-oceanic ridges and the Indian scenario

Sridhar D. Iyer* and Dwijesh Ray

National Institute of Oceanography, Dona Paula, Goa 403 004, India

We examine and synthesize the existing information about the structure, tectonic and petrology of the 70,000 km long mid-oceanic ridges and focus on similar studies made of the Carlsberg–Central Indian Ridges. The potential research areas and problems are also identified for the Indian ridge programme.

ANALOGOUS to the Great Wall of China, but several magnitudes larger in dimensions, lie the underwater mountains that form mid-oceanic ridges (MOR). Constituting ~ 23% of the earth's surface, MOR are ~ 70,000 km long with an average width of 300 km and elevated ~ 2000 m above the seafloor. They typically have high heat flow, marked seismicity and rifting along the crests¹. MOR may either intrude into the continents (Gulf of California, East Coast of Africa) or subduct below the continent (West Coast of Chile, Indonesia) or manifest as a landmass (Iceland).

The association of underwater volcanic forms and activities results in ridge (including fracture zones, FZ) and central type of eruptions; the former is confined to MOR and the latter to abyssal hills and seamounts. Certain rocks typically occur near a structural or geomorphic feature, e.g. ultramafics in transform faults (TF) and alkaline basalts at seamounts. Relationship between deep sea magmatism and the structural and tectonic features helps to understand the intensity, type and scale of volcanism and the various magmatic processes, both external (lava flow and its morphology) and internal (mantle flow, melt generation, magma segregation and migration). The advent of plate tectonic and sea floor spreading theories^{2,3} and the discovery of magnetic stripes near the Carlsberg Ridge (CR)⁴, recognized the importance of petro-tectonic studies.

Basalts are ubiquitous on the sea floor and have been variously termed: submarine basalts, sea- or ocean-floor basalts, oceanic basalts or tholeiites, abyssal basalts or tholeiites and MOR basalts (MORB). Since not all basalts erupt along MOR and not all are strictly tholeiitic, some workers call them as 'ocean-floor basalts' (OFB)⁵. MORB cover approximately 60% of the earth's surface area and are 1000 times more abundant than alkali basalt series⁶. A simple 3-layer model for the oceanic crust was proposed⁷

and subsequent geophysical surveys and geological samplings led to define these layers in terms of P-wave velocity, lithology, thickness and density (Table 1). Depending on assumptions concerning the nature of layer 3 of the oceanic crust⁸, estimates for MOR volcanism vary from < 5 km³/yr to > 20 km³/yr. This contrast with volumes of 1.5 and 1.7 km³/yr computed for hotspot and island arc volcanism respectively⁸. Annually, about 75% of the magma reaching the Earth's surface is emplaced at the MOR to produce ~ 3 km³/yr extrusives and ~ 18 km³/yr intrusives⁹. Calculations show that approximately 50 million tons/yr of OFB goes to form seamounts, but surprisingly, such a huge volume of basaltic lava corresponds to just 0.2 to 0.3% of the yearly amount of terrigenous sediments (25.33 billion tons/year) contributed by the rivers to the oceans and is also significantly less than the basalts formed (60 billion tons/year) at the MOR¹⁰.

In the young and tectonically active Indian Ocean, the MOR manifest as the Central Indian Ridge (CIR) that bifurcates into South East and South West Indian Ridges (SEIR, SWIR) and meet at the Rodriguez Triple Junction (RTJ; 25°S/70°E) (Figure 1). In the north the CIR continues as the CR that truncates against the Owen FZ near the Red Sea. The CIR is extremely segmented and offset by major NE–SW trending FZs which are common up to north of 23°S. A large number of ridges, basins and plateaus are the other distinctive features of the Indian Ocean¹¹.

In 1965, a remarkably detailed physiographic map of the Indian Ocean was published¹² and it was updated¹³ a decade later under the International Indian Ocean Expedition (1959–65; India was an active participant). The developments in remote sensing and data imaging techniques, helped delineate finer tectonic patterns, preparation of the GEBCO bathymetric charts (1975–1982) and the gravity field map of the Indian Ocean¹⁴.

Characteristics of MOR

In the study of the MOR, a frequently used term is 'neovolcanic zone' (NVZ), an area of plate boundary that witnesses recent and ongoing volcanism associated with remarkably narrow spreading center and high temperature hydrothermalism. The part of the ridge crest encompassing the NVZ has variously been described as axial

*For correspondence. (e-mail: iyer@csnio.ren.nic.in)

SPECIAL SECTION: MID-OCEANIC RIDGES

Table 1. Important parameters of the crustal structure of the oceans.
Typical values within brackets

Layer	Lithology	P-wave velocity	Thickness (km)	Avg. density (g/cm ³)
1	Sediments	1.7–2.0	< 1	2.3
2A	Basaltic sheet and pillow lavas	2.0–4.1 (3.6)	0.0–1.5 (0.5)	2.7
2B	Basaltic dykes	4.0–5.6 (5.2)	0.6–1.3 (0.9)	2.7
3A	Gabbros	6.5–6.9 (6.9)	2.0–3.0 (2.5)	3.0
3B	Layered gabbros	7.0–7.5	2.0–5.0	3.0
4	Peridotites	8.1	–	3.4

Source: BVSP⁵, Wilson²⁶.

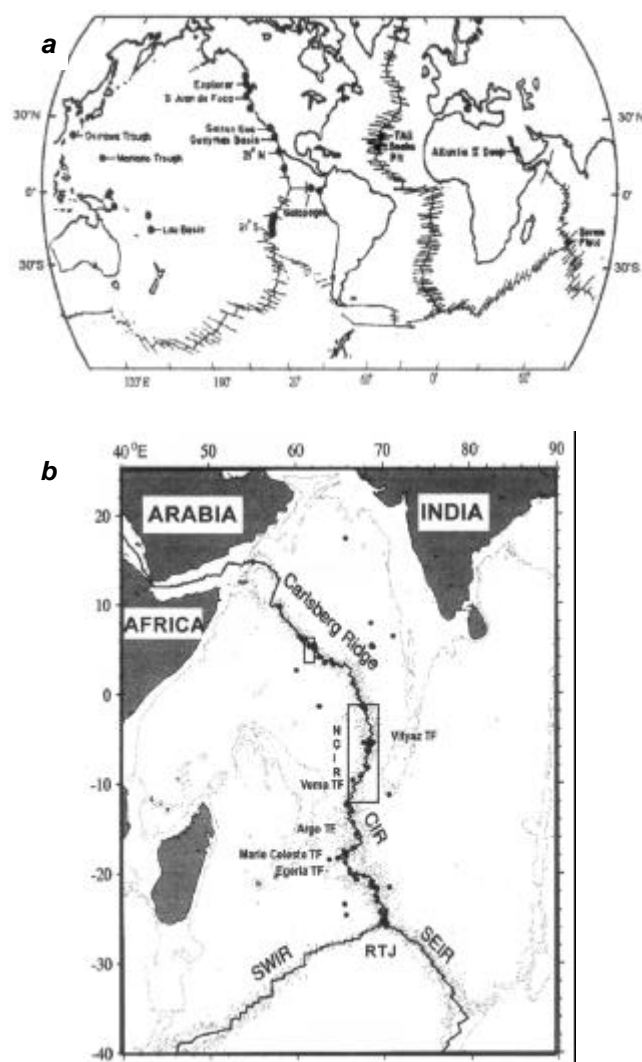


Figure 1. *a*, The global system of mid-oceanic ridges. The dark dots are sites of hydrothermal activities. Note the paucity of such sites in the Indian Ocean. *b*, Map showing the Indian Ocean Ridge System (IORS) and 125 dredge locations along the Carlsberg-Central Indian Ridge. The data have been compiled from 30 different references (data bank is available with the authors). Presently our areas of investigations are marked on the Carlsberg Ridge (CR ~ 3°N to 5°N) and the Northern Central Indian Ridge (NCIR ~ 2–12°S). The areas between 10–6°N, 4–1°N, 2–5°S, 6–9°S and 10–14°S need to be thoroughly studied. Base map has been taken from ETOPO5 map¹¹. NCIR, Northern Central Indian Ridge; CIR, Central Indian Ridge; SEIR, SouthEast Indian Ridge; SWIR, SouthWest Indian Ridge; RTJ, Rodriguez Triple Junction; TF, Transform Fault.

valley, rift valley, inner valley floor, median valley, elongate summit depression, axial summit graben and axial summit caldera¹⁵.

Spreading rate

Proponents of plate tectonic theory believe the earth's lithosphere to consist of oceanic-continental plates that either diverge, converge or subduct. MOR exemplify the former where new oceanic crust is continuously generated along a narrow axial rift valley at a variable speed, termed as 'spreading rate'.

Slow spreading ridges (10–40 mm/yr, full rate) are normally characterized by 1–2 km deep and 8–10 km wide axial valleys and have rugged faulted topography (Mid-Atlantic Ridge, MAR; Indian Ocean ridges). Areas of intermediate spreading rates (40–80 mm/yr) have 50–200 m deep and 1–5 km wide axial valleys (Juan de Fuca, Gorda and Galapagos Ridges, East Pacific Rise, EPR at 21°N, SEIR). At fast and ultrafast spreading ridges (80–160 mm/yr) the axial valley is absent (a triangular-shaped axial high is observed) and the NVZ is very narrow¹⁵ and the topography is relatively smooth with presence of horst and graben structures (EPR at 5–14°N). The NVZ at slow spreading ridges can extend across the entire axial valley floor and the lower magma supply, thicker crust and deeper extent of hydrothermal cooling lead to episodic volcanism. Under these conditions, tectonic events rather than volcanic activities are more frequent than at faster spreading ridges, because the likelihood of build-up of horizontal tensional stresses perpendicular to the ridge during ridge axis extension increases over long periods of time without interruption from volcanic activities¹⁵.

Spreading rate plays a pivotal role on the magmatic and tectonic processes and can be related to the MOR characters like width of NVZ, morphology of ridge crest, size and frequency of eruptions, form of lava flows and amount of heat transferred by an uprising magma^{15,16} (Table 2). Additionally, the spreading rate could correspond to zones of elevated temperatures and/or partial melt¹⁷. There is also a dependence of ridge-axis morphology and magma supply on spreading rate¹⁸. The occurrence of a 'local trend'¹⁹ (defined by a positive correlation

between Na₂O and FeO abundance, exhibited by MORB collected from a single ridge segment and corrected to 8.0 wt% MgO) is more likely at slower-spreading centres than at faster-spreading centres depending on whether or not a steady-state magma reservoir can be sustained at a given spreading rate²⁰. The critical spreading rate, above which a steady-state magma reservoir can form and below which one cannot, appear to be about 50 mm/yr while near this critical spreading rate a reservoir may be quasi-steady-state¹⁷.

MOR petrology

Studies on the oceanic rocks are just 125 years old since the time MAR basalts were reported²¹. Later extensive samplings have shown that basaltic lavas with unique chemical composition characterize the upper oceanic crust^{6,22,23}. We detail here the OFB in terms of morphology, mineralogy, composition, magmatic processes and alteration.

Lava morphology

Basaltic lavas erupted on the seafloor attain different forms (aa, pahoehoe and pillow flows) depending largely on the depth at which they erupt and their composition. Basalts may be vesicular and show glassy margins produ-

ced due to rapid chilling when the lava contacts seawater. Lavas commonly form pillows (10–100 cm in dia.) when bulbous protrusions of submarine flows detach from the parent flow and come to rest (while still hot and plastic) on the seafloor²⁴. Very thick flows may grade downwards from pillows into massive or columnar interiors. Although pillows form only at deeper depths due to increased hydrostatic pressure, examples of pillows associated with glassy fragmental debris at shallow depths are more common¹⁶. The pillows are progressively more crystalline towards the centre and have radially oriented joints. Vesicles are most abundant near the top and sometimes produce an amygdaloidal structure. Olivine phenocrysts may be concentrated near the bottom²². The dominant lava morphology on a ridge is clearly related to the spreading rate. For example, slow-spreading ridges almost exclusively produce pillow lavas (if sheet lavas formed earlier, it may be masked by late stage pillows) and fast-spreading ridges produce mostly sheet flows while intermediate ridges produce both but pillows predominate¹⁵.

Petrography

OFB consist of olivine, plagioclase (labradorite-andesine), pyroxene (augite), opaques (Fe–Ti oxides) and spinel. The magma composition and its cooling history are reflected by the textures and mineralogical assemblages²⁵. The grain sizes are variable (phyric to aphyric) and

Table 2. Some significant characteristics and contrasts between slow- and fast-spreading oceanic ridges

Slow-spreading ridges	Fast-spreading ridges
Spreading rate < 40 mm/yr (full rate)	Spreading rate 80–160 mm/yr
Presence of deep-seated earthquakes and major normal faults	Absence of accumulated stress and hence very less prone to earthquakes
Rough to very rough seafloor morphology	Smooth seafloor morphology
Presence of a median valley	A rise develops due to absence or poorly formed median valley
Highly segmented and asymmetric rifted depressions are conspicuous	Symmetrical and elevated volcanic edifices are present
Nature and scale of segmentation is predominantly controlled by tectonic activity	Magmatic dominates over tectonic processes
Neovolcanic zone is wider (2000–12000 m) and has small seamounts	Neovolcanic zone is narrow (100–200 m) and virtually no seamounts are present
Near-absence of off-axis seamounts	Frequent presence of off-axis seamounts
Magmatic discontinuities and unfocused magmatism	Magmatic continuity and relatively focused magmatism
A low rate of magma outpouring prevails, Volcanic eruptions are larger	The magma outflow rate is higher, Volcanic eruptions are smaller
Dykes are less but if present are large in dimension	Dykes are common are of smaller dimension
Pillow lavas abundant	Sheet flow dominant
A narrow range of relatively undifferentiated lavas are produced	A wider range of generally more differentiated lavas are present
The lavas show more complex chemical trends ascribed to polybaric fractional crystallization and/or phenocryst reaction associated with widespread accumulation of calcic plagioclase	The compositional variations are dominated by relatively simple low pressure fractional crystallization trends
Small and/or intermittent, long-lived and non-steady-state magma chambers	Large, short-lived and steady-state magma chambers
Magma mixing is most evident	Crystal fractionation largely overrules magma mixing
Mafic and ultramafic rocks commonly occur	Rare occurrence of mantle rocks

crystallinity ranges between holohyaline and holocrystalline. The presence of highly embayed phenocrysts in disequilibrium with the host magma supports the importance of magma mixing in the evolution of MORB. The commonly observed phenocryst assemblages in OFB are: olivine \pm Mg–Cr spinel; plagioclase + olivine \pm Mg–Cr spinel; plagioclase + olivine + augite. Augite phenocrysts are scarce and usually occur with abundant olivine and plagioclase. Olivine, spinel and calcic plagioclase crystallize first followed by augite and Fe–Ti oxides. Amphibole is very rare, occurring only in basalts with alkaline affinities and in cumulate gabbros²⁶.

Olivine is usually euhedral but more anhedral in pyroxene-rich rocks. The phenocrysts may be moderately zoned and in many cases the cores are too Mg-rich to be in equilibrium with the bulk rock, attesting to their derivation from a more mafic source by magma mixing. Depending on the magma composition, the phenocrysts range from Fo₇₃ in ferrobasalts to Fo₉₁ in picrites. Clinopyroxene phenocrysts are colourless to pale green diopsidic augite with restricted chemical composition (Wo_{35–40} En₅₀Fs_{10–15}) and subcalcic augite and Mg–pigeonite are rare²⁶. Plagioclase ranges from An₈₈ to An₄₀ and a negative relation between An content of early formed plagioclase and spreading rate could exist²⁷.

In general, normal (N) and enriched/plume (E/P) MORB are different in their chemistry, indicating varying magma composition and crystallization condition. In N–MORB, plagioclase is usually the dominant phenocryst accompanied by olivine and near absence of pyroxene while E–MORB are olivine and pyroxene phyrlic. Depending on the crystallization history, two basaltic tholeiites have been identified: olivine and plagioclase²⁸; whereas based on petrography, order of mineral crystallization and relative mineral proportions, six basaltic types were recognized: picritic, highly phyrlic plagioclase basalts; moderately phyrlic plagioclase, plagioclase–olivine–pyroxene, olivine bearing and plagioclase–pyroxene²⁹. Some difficulties may arise if the rock is dominantly aphyric (glassy). Glass being compositionally more consistent, better represents the original magma chemistry and helps to compare basalts from diverse regions. To understand the liquid line of descent of the remaining magma, the effect of plagioclase and/or olivine phenocrysts in the glass need to be removed.

Chemical composition

Early studies emphasized the unique and near-uniform chemistry of OFB and in particular their tholeiitic nature: constant Si values, low K abundances, low K/Na ratios, low magmaphile element content and high K/Rb ratios^{6,22}. Rocks recovered through drilling, dredging and by using submersibles, indicate the compositional and petrological diversity at a single site to be more frequent than was believed³⁰.

OFB have low K, Ba, P, Pb, Sr, Th, U and Zr contents and are similar to basaltic achondrite⁶ as also attested by REE and K–Rb contents. The major elements Si, Al, Fe, Mg, Ca and Na play an important role, while Ti sometimes qualifies and at times behaves purely as a trace element. SiO₂ has a narrow range (49–52%) and covaries with the abundance of Mg and Fe. Plagioclase accumulation (CaO 11–12%) causes an enrichment in Al content. The least evolved basalts have MgO of 10–11% and Fe 8% and Mg# 68–71 (Mg# = 100 \times MgO/[MgO + FeO*], atomic proportion) while the most evolved basalt contains MgO as low as 6% and Fe up to 13.5% with Mg# 45. TiO₂ (0.7–2%) acts as an incompatible trace element in the more magnesian lavas but in the Fe-rich ones it occurs in an oxide phase and/or in amphibole^{26,31}. Tables 3 and 4 show the typical compositions of OFB.

MORB are depleted in K and Rb and as K decreases, K/Rb increases to over 1000 from the values of a few hundreds which is more common in basalts from other settings⁶. Cr and Ni are strongly partitioned into solid phases and provide vital information of the melting and crystallization processes. For example, Cr and Ni decrease with advancing fractional crystallization, i.e. with increasing FeO*/MgO ratio. In the more magnesian basalts, Cr ranges between 550 and 600 ppm and falls with decreasing Mg#. Both Ni and Cr enter early-stage mafic mine-

Table 3. Major element compositions of basalts from three world oceans. MIOR, Mid-Indian Ocean Ridge; MAR, Mid-Atlantic Ridge; EPR, East Pacific Rise

Oxides	MIOR	MAR	EPR
SiO ₂	50.93	50.68	50.19
TiO ₂	1.19	1.49	1.77
Al ₂ O ₃	15.15	15.60	14.86
FeO _t	10.32	9.85	11.33
MgO	7.69	7.69	7.10
CaO	11.84	11.44	11.44
Na ₂ O	2.32	2.66	2.66
K ₂ O	0.14	0.17	0.16
P ₂ O ₅	0.10	0.12	0.14

Source: Melson¹⁰⁵.

Table 4. Trace element compositions of basalts from three world oceans

	MIOR ^{a,b}	MAR ^{b,c}	EPR ^{b,c}
Rb	2.54	2.24	1.4
Sr	141	116	120
Ni	106	121	100
Cr	320	300	318
Co	42	49	47
Cu	81	77	78
Y	35	25	39
Zr	112	46	88
Nb	4.0	1.6	2.0
V	243	289	318

Source: a, Banerjee and Iyer⁴²; b, Subbarao *et al.*⁸³; c, Sun *et al.*¹⁰⁶.

erals, particularly olivine. Cu and Zn show little variations at the magmatic stage, about 100 ppm for both³¹, while the more evolved liquids have < 50 ppm Cu and 150–200 ppm Zn.

To summarize, the OFB markedly have very low K₂O and low TiO₂, total iron, P₂O₅ and Fe₂O₃/FeO while CaO is high. Atomic abundances of Ba, Sr, Rb, Pb, Th, U and Zr are low to very low and so also Th/U and ⁸⁷Sr/⁸⁶Sr (0.7029 to 0.7035), whereas K/Rb ratio is exceptionally high (700 to 1700). Normative calculations show OFB to range from alkali tholeiites (with a few percentage of normative nepheline) to quartz-tholeiites (with few percentage of normative quartz). But mostly the basalts are olivine–tholeiites or transitional basalts with a few percentage of normative–hypersthene.

Geochemically, the MORB can be divided into three types^{23,32}: N, E/P and transitional (T). About three-fourths of the MOR hosts N–MORB, an estimation based on the observation that 17 ridge centered hotspots with an average length of 1000 km occur along the MOR³³. N–MORB are depleted in incompatible and light rare earth elements (LREE) and have high K/Ba, K/Rb, Zr/Nb and low ⁸⁷Sr/⁸⁶Sr. Geochemically, E–MORB are remarkably similar³⁴ having moderately elevated K₂O (0.10–0.30% at Mg# > 65), low Zr/Nb and Y/Nb (6–16 and 1–4, respectively) and enhanced (La/Sm)_N ratios (1–6; N denotes chondrite normalized). Further, the E–MORB are richer in high field strength elements (U, Th, K, Rb, Cs, Ba, Nb, LREE, P, Ta) and Sr and Pb isotopes than N–MORB and have (La/Sm)_N > 1. But K/Ba, K/Rb, La/Ce and Zr/Nb ratios are lower than those of N–MORB and comparable to oceanic-island tholeiites. These features contrast with those commonly associated with depleted N–MORB^{5,34} [i.e. K₂O typically < 0.15 wt% at Mg# > 65; Zr/Nb > 16; Y/Nb > 8; (La/Sm)_N < 1.0)] and thus suggest different sources for the two types.

At a given MgO value, lavas from slow-spreading ridges generally have greater Na₂O, Al₂O₃ and lower FeO and CaO/Al₂O₃ contents than those from fast-spreading ridges. To decipher the petrogenesis^{18,19,35}, the chemical variations are expressed as Na₈, Fe₈, Ca₈ and TiFe_{7,3} which are calculated at a constant MgO content (7–8.0 wt%).

Magmatic processes

Compositionally, the erupted basalts may be quite different from its parental source produced at depth. An ascending magma loses heat, crystallizes minerals and reacts with the wall rock through which it migrates. Interestingly, MORB derived from varying depths reach the surface with broadly comparable major-element compositions. The only fact that can confidently be concluded from the normative compositions is that nepheline-normative MORB were probably derived from a depth > ~ 30 km from liquids that lie on the silica-deficient side of a thermal divide¹⁵.

The chemical variations within suites of associated rocks dredged from the MOR or seamounts are increased Fe/Mg ratios, SiO₂, TiO₂ and most REE and decreased MgO, Al₂O₃, Ni, Co and Eu, all of which indicate fractionation in a very shallow reservoir and confirm the petrographical observations²⁰. Olivine and plagioclase critically affect the low pressure fractionation as evident from the rapid depletion of Ni with escalating differentiation and significant negative Eu anomalies in an otherwise unfractionated but highly enriched REE pattern⁵.

MORB glasses with low Na_{8,0} define low pressure liquid lines of descent (LLD) while higher crystallization pressures and greater variability are obtained from slow- and medium-spreading ridges. Crystallization pressures do not vary uniformly along individual segments. The correlation between average crystallization pressure and Na_{8,0} suggests that magma supply (and perhaps mantle temperature) may constrain its ascent and crystallization depths. Not surprisingly, fast-spreading ridges have relatively lower average pressures of crystallization, but slow-spreading ridges have a range of pressures³⁶. Hence, lavas from the latter are not well fractionated and fall on poorly defined LLD^{27,37}, suggesting high pressure (3–6 kbar) or *in situ* crystallization^{38,39}. Variations in MORB can be ascribed to shallow depth of differentiation²² dominated by plagioclase and olivine while the major characteristics are indicative of extensive partial melting (~ 30%) at lesser depths (15–25 km).

Compared to olivine and plagioclase, clinopyroxene saturation temperature largely depends on pressure (i.e. a greater dP/dT). Hence, higher pressure favours earlier saturation of clinopyroxene resulting in decreasing CaO and MgO. Most MORB display this trend and must have crystallized clinopyroxene at some point during their evolution. However, it is absent in many fractionated lavas and is demonstrably unstable in many liquids at low pressures³⁶. This ‘pyroxene paradox’ is attributed to crystallization at higher pressures followed by magma ascent and dissolution or segregation of clinopyroxene during olivine + plagioclase crystallization³⁸. *In situ* crystallization, whereby evolved liquid from a highly crystallized boundary layer is expelled and mixed with more primitive liquid, could also explain the lack of clinopyroxene, despite its participation in generating their LLD³⁹. Hence, a basaltic liquid could pick up the signature of clinopyroxene crystallization (low CaO at a given MgO content) even at low pressures, yet not be saturated with pyroxene³⁶.

A review of the main geochemical evidences bearing on mantle structure and processes and some models based on it, led to the conclusion that much of the chemical heterogeneity seen in MORB is due to recycling of oceanic and to a much lesser extent continental crustal material, which resurfaces predominantly in the mantle plume that create volcanic islands⁴⁰. It was opined that the uppermost mantle, the source of MORB, is depleted in incompatible

elements by (i) devolatilization and melting during subduction transfer incompatible elements to long-time (or permanent) storage in the continental crust and lithosphere and (ii) a portion of the subducted oceanic crust is stored at the base of the convecting system and thus sequesters incompatible elements temporarily and the remainder of this crust is mixed back into the MORB reservoir⁴⁰.

Source heterogeneity is an important factor in MORB petrogenesis along with fractional crystallization, magma mixing, variable degrees of partial melting and fluctuating residual source mineralogies²⁶. N-MORB are derived by partial melting of the isotopically fairly homogeneous, well-mixed, depleted upper-mantle reservoir, whereas E-MORB are from a more enriched plume (hotspot) from the underlying isotopically heterogeneous reservoir.

Magma mixing

To explain the large differences in trace element abundances seen in otherwise similar OFB, a model was forwarded involving fractionation of mixed magmas⁴¹ that is supported by mineralogical, geochemical and experimental evidences⁵. For example, the indications registered in the CR basalts that imply magma mixing prior to final cooling are: low CaO/Al₂O₃ ratio in the bulk rock compositions, near absence of clinopyroxene and hyperbolic relation of the ratio–ratio plots of trace elements, variable TiO₂ at a given FeO*/MgO, coexistence of calcic plagioclase and olivine with minor compositional variations of the latter and varied morphology and composition of plagioclase^{42,43}.

Although magma mixing could explain the variation in closely associated OFB compared to crystal fractionation, it cannot account for the large range of incompatible element ratios. These may in fact be related to complex melting processes³⁹ or source inhomogeneities⁴⁴. The latter has been noted at the accreting plate boundaries of the MAR^{23,30}, at parts of the Central Eastern Pacific⁴⁵ and in the CR and CIR^{46–49}. Significant differences in sources and melting parameters could control the MORB composition on a regional basis while local chemical variations may primarily be restricted by fractionation and magma mixing at shallow level.

Detailed seafloor mapping, compositional data and quantitative models assist to examine the volumes, rates of eruption and ranges of geochemical variation within several individual lava flows erupted on the MOR¹⁵. The data are consistent with a model in which fast-spreading ridges have frequent, relatively homogeneous, small volume eruptions *vis-à-vis* slow-spreading ridges (Table 2). The key effect, on the variables that change with spreading rate along the MOR system, seems to be whether or not a steady-state magma reservoir can be sustained at a given location. Where magma supply is

continuous and robust, volcanic output dominates over tectonic processes; where the supply is intermittent, the latter dominates. The critical spreading rate between steady-state and non-steady-state magma reservoirs is approximately 50 mm/yr (ref. 15).

Extensive samplings reveal primitive lavas to occur at the central elevations of ridge segments, while progressively more evolved lavas erupt at a distance¹⁵. This may be due to tapping of a zoned magma chamber that was continually evolving and periodically recharged⁵⁰. Samples proximal to TF and/or associated with propagating rift tips show these areas to exemplify extensive fractionation of magmas due to relatively cooler thermal regimes.

Magma chamber

The chemical and mineralogical diversity of MORB may be accounted by assuming the presence of a magma chamber beneath the MOR. Although it is inevitable that an ascending magma would form stationary pools in the crust prior to its eruption, very little is known about the size and shape of such pools or chambers despite a variety of theoretical models. Geophysical evidences support the concept of persistent magma chambers but due to the buffering process, such magma chambers need not necessarily be large⁵¹.

Axial magma chambers may exist as a closed system or more commonly as a periodically replenished open system. The size and persistence of magma chambers being intimately related to the spreading rate, as the latter increases above the critical value the chamber must expand in size until at a half-rate of 60 mm/yr it will underlie 10 km of ocean floor on either side of the ridge axis⁵². Thus, fast-spreading ridges may host large continuous magma chambers, whereas slow-spreading ridges will have small discontinuous reservoirs.

Seismic velocities indicate small mush zones of several kilometers to occur beneath slow-spreading ridges⁵³ rather than large sub-axial magma chambers⁵⁴. The 'infinite leak' model explains the crustal formation at slow-spreading ridges, assuming that no permanent sub-axial magma reservoir exists⁵⁵. In this model magma rises to high levels by a process of crack propagation through the brittle crust, allowing the existence of only very small storage reservoirs.

The magma chamber configuration has been redefined as 'relatively small (< 1 km thick, 1–3 km wide), tectonically bounded, lenticular magma chambers surrounded by semi-molten low-seismic-velocity zone'³⁷. Reports suggest that proximal to structural offsets, such as transform faults, a lower magmatic temperature and a wide range of magma composition exist resulting in eruption of E-MORB⁵⁶. Thus, TF could separate coherent geochemical units reflecting differences in crystal fractionation and extents of melting. A concept of 'spreading cell-

deval⁵⁶ has been proposed to account for an observation of such small magma chambers. (A small ridge portion bounded by two transform faults is known as a spreading cell that also describes the boundary of smaller magma chambers, 'deval'—deviation from axial linearity.)

A general source of MORB is depleted lherzolite in the spinel or possibly even plagioclase lherzolite facies²⁶. Partial melting of more enriched mantle sources apparently generates some MORB associated with topographic highs along the MOR axis. Experiments on synthetic and natural lherzolites indicate that a minimum of ~20% partial melting is needed to generate the most primitive (MgO-rich) MORB. If primary MORB are more picritic, then the degree of melting would be somewhat greater. The decline of P and S waves suggests the start of significant partial melting in rising mantle diapirs at depths of 60–80 km. Mantle peridotites with Mg# < 88 produce primitive MORB by 15–20% partial melting at 1.0–1.5 GPa followed by small amounts (a few to 10%) of olivine fractionation, while those with Mg# > 89 produce primitive MORB by partial melting at pressures > 1.5 GPa followed by extensive olivine fractionation⁵⁷.

Magmatic and tectonic segmentation

Tectonic and magmatic segmentations of MOR occur at several scales that overlap or form a continuum. It is presumed that segmentation is hierarchical and is an outcome of mantle flow and upwelling patterns⁵⁸. The largest scale of magmatic segmentation is isotopic, reflecting differences in mantle history and composition spanning a range of scales as large as individual ocean basins or larger. This could be superimposed by large transforms and/or non-transforms offsets that could reflect differences between slow- and fast-spreading magmatic segments, although magma supply, plume influence and ridge obliquity may also have important effects⁵⁸.

In contrast to the view that the generation of the oceanic crust is a steady state process producing MORB of essentially constant composition through time, detailed studies conducted at the segment length scale have linked patterns of compositional variability at the EPR and at the southern Juan de Fuca Ridge⁵⁹. An orderly spatial zonation of N- and T-MORB around a 50 km length of the EPR axis suggests the possibility of geochemical stripes of the seafloor³⁵. These stripes will be asymmetrical because of changes in segmentation that occur during the progressive temporal changes in composition, perhaps with some irregularities resulting from off-axis eruptions. Since the temporal changes in magma chemistry take place over 10⁴ years, they provide potentially an order of magnitude finer resolution than the magnetic reversals that occur at 10⁵ to 10⁶ years. Geochemical stripes, in combination with bathymetry and better radio-

metric dating may reveal the history of fine-scale petrologic and structural segmentation of the sea floor³⁵.

Submarine alteration

Interaction of seawater and OFB would result in different degrees of weathering, metamorphism, hydrothermal circulations and deuteric compositional changes brought during and after magmatic solidification. Weathering of an outcrop depends on presence of joints, fractures and fissures and on its mineralogy and age, among others. The resultant alteration products help understand the formation of authigenic minerals, chemical budget of seawater, circulation of fluid in the crust, type of tectonic activity involved and nature of transport and redeposition of materials extracted from the basement rocks⁶⁰. During alteration OFB undergo physical, mineralogical or chemical changes or exhibit all of these. A most prominent and easily identifiable change is in the colour, grading from medium to light gray with brownish tinge glassy top, through a dark gray to a medium light gray interior⁶¹. Seawater interaction generally hydrates the rock, reduces the density, affects acoustic properties and decreases magnetic susceptibility while porosity is reduced by infilling of cracks, pores and voids⁶².

Mineralogical variations depend on the material altered. The homogeneous basaltic glass alters continuously while the multiphase crystalline interior is altered stepwise such that the matrix of cryptocrystalline and glassy material alter first together with the filled vesicles. The common alteration products are palagonite, chlorite, chlorophaeite, celadonite, zeolites (phillipsite, harmotome), montmorillonite and iron oxides and hydroxides. Titanomagnetite is altered to maghemite during early alteration, olivine to hydrated Fe-oxides, iddingsite, limonite and smectite, while plagioclase (less altered to smectite and sericite) and pyroxene are most resistant.

Compositional changes indicate that relative to seawater, altered OFB act as source or sink for various elements. For example, OFB release Si, Mg and Ca and trap Ti, K, P, Mn, Fe, Na and H₂O from the seawater, while Al shows no conclusive exchange. Fresh basalts have low oxidation ratio (Fe₂O₃/FeO + Fe₂O₃ < 0.55) but altered ones record high values (> 0.55). From the H₂O and Fe₂O₃ contents, a scale for various stages of alteration was devised⁶³: unaltered (H₂O 0.3), partially altered (H₂O 0.4–0.7), altered (H₂O 0.6–0.7; Fe₂O₃ 0.2–0.3) and highly altered (H₂O 1.0). Alteration is also characterized by varying enrichments in B, Li, Rb, U, and Cs and sometimes in Sr, Ba, and LREE *vis-à-vis* Sc, V, Co, Y, Zr, Ti, heavy REE that are least affected⁶¹. Low temperature alteration predominates and results in rapid palagonitization of the basaltic rims than of the interior⁶⁰, while high temperature alteration leads to metamorphosis.

Central Indian Ridge (CIR)

Very few studies have been carried out along the CIR including the expeditions of *Monsoon* 1960, *Lusiad* 1962–62, *Dodo* 1964, *Circe* 1968, *Antipode* 1970–71 and Deep Sea Drilling Program (DSDP) in 1972 (Legs 22, 24, 26 and 27).

The CIR, an intermediate-to-slow-spreading ridge that began to form during the Late Cretaceous, is highly segmented by NE–SW trending FZ^{11,64,65} and part of it (south of 10°S) is the accreting plate boundary of the Australian Plate (or the Capricorn plate) in the present day five (or six) plate geometry (Antarctic, Australian, African (Somalian), Arabian, Indian and possibly Capricorn plates) of the Indian Ocean^{66,67}. The Wide Boundary Zone or Diffuse Plate Boundary separates the Indian and Australian plates and intersects the CIR between 4 and 9°S. It was speculated that the regular spacing of the discontinuities on the CIR are controlled by magmatism⁶⁸.

The CIR spreads at 27 mm/yr, SEIR at 30 mm/yr and SWIR at 6.5 mm/yr (all half-spreading rates). The spreading rate from north to south ranges⁶⁴ between 18 and 24 mm/yr. According to Price *et al.*⁶⁹, the spreading rate of the SWIR is < 10 mm/yr; CR ~ 13 mm/yr; CIR ~ 18–25 mm/yr and SEIR ~ 30–36 mm/yr. The present day spreading rate and direction progressively change⁶⁶ between the RTJ (55 mm/yr, N152°E) and the equator (34 mm/yr, N142°E). Magnetic and bathymetric data across five ridge segments (N50°E profiles) of the Vema (7–12°S, 64–70°E) reveal asymmetric spreading uptill chron A5 (10 Ma). Although inter-segmental variation in the rate exists, the mean spreading rate increases from 18 mm/yr north of Vema to 21 mm/yr south of the Vema⁷⁰.

The area between 18° to 22°S and 66° to 69°E reveals a NW–SE trending median valley associated with broad and high-amplitude magnetic anomaly (2, 2A, 3, 3A and 4) along the ridge crest and a rate of 44 mm/yr is estimated for the last 10 Ma. A ridge jump between the anomalies 2-2A (approx. 2.5 Ma) and a lateral transform fault offset the ridge axis by about 50 km (ref. 71). Multibeam studies (7°30′–8°30′S) helped identify a TF at 7°45′S that offset the ridge axis by 30 km and a variable along-axis crustal thickness⁷². The complex seismicity and bathymetric pattern of the CIR from the equator to 7°S is because of short ridge segments and small offset transforms⁷³.

GLORIA long-range side-scan sonars studies (12°S and 24°S) exhibit a well-defined distribution of the CIR axis into five spreading ridge segments⁶⁸. Each segment (length 275–390 km, av. 322 km) is characterized by a particular structural style of axial spreading ridge and separated from its neighbour by major (or master) FZ. Within this large-scale structural segmentation, the megasegments are further subdivided into 14 higher order segment boundaries, separated by between 18 km and ~ 100 km of the CIR. The regional trend of the CIR is

largely inherited from those prevailing prior to magnetic anomaly 20 ± 45 Ma) and the present geometry was established during the plates reorganization when India and Eurasia collided⁶⁸.

Along the Sheba, CR and CIR, the FZ strike N50°E to N60°E. From northwest to southeast, a number of FZ occur: Alula–Fartak FZ at the mouth of the Gulf of Aden; Owen FZ separating the Sheba Ridge from the Carlsberg Ridge, fracture zone at 3°N, the Mahabiss FZ, Sealark FZ, Vitiaz FZ, Vema FZ, Argo FZ, Marie Celeste FZ and Egeria FZ and Gemino FZ which lies east of the Rodrigues Ridge. Except for the Alula–Fartak FZ and the FZ at 3°S, all the offsets are left-lateral with the largest being located along the Alula–Fartak FZ (200 km), the Owen FZ (300 km), the Vema FZ (200 km) and the Marie Celeste (220 km) (ref. 74).

CR–CIR petrology

In 1935, CR basalts were first recovered and described⁷⁵. Thirty years later ‘Expedition Dodo’ (Scripps Institution of Oceanography) dredged between 23° and 24°S (water depths 3700 to 4300 m). During the seventies, the DSDP drilled at 21 sites (211–216, 231–238, 253, 254, 256, 257, 259–261) and collected basalts and related rocks from the CR, CIR, Somali Basin, Ninety East Ridge, etc. In 1987, the Ocean Drilling Program (ODP) utilized the ‘Resolution’ of the JOIDES (Joint Oceanographic Institutions for Deep Earth Sampling) to explore the volcanic, oceanographic and plate tectonic history of the western and Central Indian Ocean and reconstruct the plate positions and volcanic history⁷⁶.

In about 60% of the more than 4,500,000 km² of the CIR, SEIR and SWIR, faulting or volcanism exposes rocks of the crust, lower crust and possible upper mantle. Rocks mainly from the major TF (Vema, Argo, Marie Celeste and Melville) were obtained from 56 dredge hauls. Studies indicate that under a capping of young flow basalt, there is a regional complex of igneous rocks produced by magma under the ridges, trapped and differentiated into sill-like, podiform, and larger, crudely stratified to well-stratified sheets⁶⁵. The rocks include abundant lherzolite and minor harzburgite, orthopyroxenites, olivine- and two-pyroxene gabbros, Ti-ferrogabbros, norite and anorthosite. Some associated diabase intrusions are granophyric and are cut by late-stage dikelets of quartz monzonite and Na-rich trondjemite. Both calc-alkaline and alkalic lines of differentiation are indicated. The overlying basaltic pillows with chemical (low-K) and mineralogical (plagioclase-rich and olivine) characteristics are typical of olivine-bearing tholeiite from the other MOR. The CIR basalts correspond more closely to type II tholeiites (Na₂O ~ 2.5–3.4; TiO₂ ~ 1.1–1.5) compared to type I (Na₂O ~ 1.4–2.2; TiO₂ ~ 0.6–1.3, DSDP 212, 236) and type III (Na₂O ~ 3.6–4.4; TiO₂ ~ 1.3–1.9, RTJ, SWIR)⁶². Incidences of

granitic rocks and lherzolite, harzburgite, gabbros and diabase come from within the deep Argo FZ.

In the light of ridge segmentation, petrological studies of nine sites (Owen FZ to RTJ) were made along the 4200 km long CIR⁷⁷. The ultramafics (serpentinized peridotites, talc-anthophyllite, lherzolites) display vertical displacement and dynamic metamorphism effects as seen from slickensides, breccias and calcitic cements⁷⁸. Isotopes and REE of rocks from different areas of the Indian Ocean ridges point to diverse magmas and magma mixing processes^{46,47,49,69,79–83}. Moreover, the length and offset of the segments may have influenced the variable extent of melting of the source rock and depth of magma generation below each segment⁷⁷.

Basalt

The area between 23° and 24°S with no median valley but high heat flow and quite fresh lava indicate abundant recent low-K tholeiitic volcanism⁶. The CIR shows compositional variations primarily caused by growth and redistribution of Ca-rich plagioclase. The enhanced ⁸⁷Sr/⁸⁶Sr ratios point to a source depleted in alkalis more recently and/or to a lesser degree than that in the MAR and EPR⁸². The depletion in large ion-lithophile elements (K, Rb, Sr, Cs, U) is probably due to partial melting at different depths and at different degrees since the geological past⁸³. The younger basalts from the CR are distinct from those at CIR, implying that the western Indian Ocean MORB require major differences in the source composition and evolution relative to the Pacific and Atlantic MORB^{77,79–81,84}.

In 1983, during Indo-Germany GEMINO-I cruise (SO-28) in two intermediate-spreading ridge segments (21.5°S area EX/FX and 23°S area JX), hydrothermally influenced sediments and altered basalts were found⁸⁵. Pillow lavas with striations and protuberances are copious near the rift valley whereas, fresh, glassy sheet flows, comprising lobate, scrambled and curtain-fold forms, predominate within the central NVZ. In area JX, fresh pillow lavas and sheet flows with glass up to 1 cm thick occur with little sediment cover. In both areas, pillow fragments and talus are > 90%, the remaining being sheet flows. The plagioclase phyric basalts have varying TiO₂ (0.7–1.5%) and K₂O (0.06–0.34%) at a given FeO/MgO ratio, indicative of multiple parental magma⁸⁵.

The CIR basalts from nine sites bear signatures of polybaric crystallization with the accumulation of and zoning in calcic plagioclase phenocrysts, suggesting an origin from small, buoyant magma chambers⁷⁷. Again, the variable presence of olivine and plagioclase in the basalts from diverse sites, points to source inhomogeneity brought about by changes in the depth of magma generation, extent of partial melting or degree of crystal separation²⁷. The concept of spreading cell could explain the differential extent of partial melting coupled with variable depth of magma generation beneath each ridge segment. The

different degrees of cooling, fractionation and segregation of magmatic melts may have resulted in a disparity in the CIR MORB mineralogy (abundant plagioclase, olivine) and texture (phenocrystic, zoning, melt inclusions).

SO-28 samples (6.15°N to 21.39°S and 60.85°E to 68.78°E) have distinct trace element signatures and correlations hinting at residual heterogeneities that have not been completely rehomogenized by convective stirring of the shallow asthenosphere. Correlations among Nb/U, Nd/Pb, Ba/Nb and Ba/Th with Sr isotopes show the distinctive isotopic signature of Indian Ocean MORB that was probably brought about by the addition of recycled sediments to an ordinary MORB source reservoir⁸⁶. Fresh basalts near the Egaria FZ (20°12'S/66°53'E) have plagioclase (An 89–78) and olivine (Fo 90–85) with melt inclusions. From least square and mass balance calculations it is postulated that these basalts were derived from a near-primitive parental basalt⁸⁷.

Gabbro

Gabbro, an integral part of oceanic layer 3, constitutes ~ 60–70% of plutonic rocks. Occurrence of gabbro and pyroxenite in a core from the Indian Ocean has been reported⁸⁸. Olivine gabbro, dominant along the CIR between 5° and 28°S, are of four types: olivine–augite gabbro, augite–hypersthene gabbro, ilmenite–magnetite rich gabbro (Ti-ferrogabbros) and albitised–hornblende gabbro⁸⁹. Olivine–augite gabbro (65% plagioclase An₈₀, 30% augite, 5% olivine) is present in Vema and Marie Celeste FZ. Augite–hypersthene gabbro (67%, plagioclase 16%, clinopyroxene 16.6% opaques) with low CaO, high Na₂O and Al₂O₃ than olivine–augite gabbro is found in Argo FZ. Gabbro composition of the CIR suggests longitudinal injection of magma from central magma chambers and from a melt more fractionated than that which forms basalt⁹⁰.

Petrological evidences together with ophiolite analogue studies, hint at the persistence of basaltic magma chambers at shallow levels immediately beneath the MOR and that gabbros and related cumulate rocks of layer 3 crystallized from these magmas⁵. Steady-state refilling and mixing of these magma bodies with batches of fresh magma would tend to retain the magma near to multiple-saturation throughout its crystallization history, producing gabbroic rocks⁴¹.

Ultramafic rocks

These were dredged from all the major FZ and are lherzolite (olivine + enstatite + diopside ± plagioclase) followed in abundance by serpentinized harzburgite and minor orthopyroxenite. It was assumed that mantle lherzolite rising into axial parts of the ridges partially melts to produce liquid basalt and residual harzburgite⁶⁵.

Isotope

One of the most interesting observations is that the melt beneath the Indian MOR is not only isotopically distinct from that in the other oceans but notable variations also occur⁶⁹. The 1350 km wide isotopic anomaly on the CIR is inconsistent with a hotspot at Reunion Island which is currently active but is more than 1000 km to the west⁹¹. Subbarao and Hedge⁸² and Hedge *et al.*⁹² were the first to conclude that the Indian MOR were fed by distinctive mantle sources. Studies of CIR basaltic glasses allude to the existence of a major isotopic province that is fundamentally different from those of the SWIR, RTJ and SEIR⁹³.

The Indian Ocean MORB are characterized on average by higher $^{87}\text{Sr}/^{86}\text{Sr}$ and lower $^{206}\text{Pb}/^{204}\text{Pb}$ and $^{143}\text{Nd}/^{144}\text{Nd}$ than the North Atlantic and East Pacific MORB (Table 5). In addition, $^{207}\text{Pb}/^{204}\text{Pb}$ and $^{208}\text{Pb}/^{204}\text{Pb}$ are higher at a given $^{206}\text{Pb}/^{204}\text{Pb}$, than in other oceanic regions⁹³. These distinctive isotopic signals have been attributed to the influence of Dupal components from the Kerguelen Plume^{81,94} perhaps with additions from Crozet and Marion plumes⁹³. The alternate view is that ancient continental lithosphere was dispersed and incorporated into the Indian Ocean MORB source during the Gondwanaland breakup⁹³. The Dupal anomaly may also suggest large-scale mantle processes or delamination of the subcontinental lithosphere⁹⁵.

Present and future research trends

The CR–CIR and Andaman Back-arc Basin are viable areas for further investigations due to a number of factors including abrupt changes in spreading rate and direction within a short distance, uneven segmentation and geo-physical, geomorphological, geochemical characteristics and micropalaeontological evidences for possible hydrothermal activities^{70,96–104}.

The InRidge program, the Indian initiative for ridge research founded at the National Institute of Oceanography in the late nineties, focuses on three areas: CIR, CR and Andaman Back-arc Basin. Multi-disciplinary studies of these areas have been carried out. Due to keen interest by the international community, the need for a CR–CIR working group was suggested⁹⁶ to address the upper mantle variability and upwelling, locus and amount of magma production, modes and rates of melt delivery to lithosphere and crust, alteration processes, hydrothermal circulation, relation between hydrothermal vents and palaeotectonics and variation of chemosynthetic and biogeographic provinces with the tectonic setting¹⁰⁰.

Besides the above, some key aspects to be studied by the ridge community are: 1. Global structure and fluxes: Details of the structure and geochemical, biological and energy fluxes of the MOR; 2. Crustal accretion variables: Assess the influence of spreading rate and magma supply on crustal accretion process; 3. Mantle flow and melt

Table 5. Isotopic ratios in ocean basalts from three world oceans. Indian Ocean basalts are characterized by high $^{208}\text{Pb}/^{204}\text{Pb}$ and $^{87}\text{Sr}/^{86}\text{Sr}$, low $^{143}\text{Nd}/^{144}\text{Nd}$ and $^{206}\text{Pb}/^{204}\text{Pb}$ contents

	MIOR	MAR	EPR
$^{87}\text{Sr}/^{86}\text{Sr}$	0.7032–0.7035 ^a 0.70261–0.70278 ^b 0.70291–0.70329 ^c 0.70273–0.70356 ^d 0.70257–0.70289 ^e	0.70230–0.70321 ^b 0.70215–0.70287 ^f	0.70253–0.70275 ^b 0.7023–0.7028 ^g
$^{206}\text{Pb}/^{204}\text{Pb}$	18.43–18.75 ^b 17.307–18.019 ^c 17.898–18.839 ^d 18.000–18.157 ^e	17.84–19.28 ^b 17.829–19.437 ^f	18.43–18.56 ^b 17.721–18.726 ^f 18.0–18.8 ^g
$^{207}\text{Pb}/^{204}\text{Pb}$	15.43–15.49 ^b 15.505–15.563 ^c 15.437–15.604 ^d 15.443–15.472 ^e	15.46–15.59 ^b 15.439–15.586 ^f	15.44–15.49 ^b 15.309–15.514 ^f 15.3–15.6 ^g
$^{208}\text{Pb}/^{204}\text{Pb}$	38.01–38.19 ^b 37.214–37.838 ^c 37.820–39.077 ^d 37.772–38.001 ^e	37.33–38.83 ^b 37.418–38.913 ^f	37.64–38.07 ^b 37.029–38.805 ^f 37.0–38.8 ^g
$^{143}\text{Nd}/^{144}\text{Nd}$	0.51302–0.51305 ^b 0.51304–0.51309 ^c 0.51293–0.51316 ^d 0.51305–0.51309 ^e	0.51309–0.51329 ^b	0.51302–0.51313 ^b 0.51306–0.51318 ^g

Source: a, Subbarao and Hedge⁸²; b, Cohen *et al.*¹⁰⁷; c, Price *et al.*⁶⁹; d, Mahoney *et al.*¹⁰⁸; e, Rehkamper and Hoffmann⁸⁶; f, Hamlein *et al.*¹⁰⁹; g, Batiza¹¹⁰.

generation: Discern their nature beneath MOR through field and laboratory experiments; 4. Event detection and response: Develop a useable and reliable event detection and response capability to identify, locate and characterize volcanic and seismic areas; 5. Temporal variability of ridge crest phenomena: Initiate a seafloor observatory programme and delineate a test site for utilisation of seafloor instruments; 6. Biological studies: Biogeography, ecology, micro-biology and astro-biology.

1. Iyer, S. D. and Mukhopadhyay, R., Underwater mountain chains, *Indian Express (Sci. Express)*, 21 Sep. 1999.
2. Dietz, R., Continent and ocean basin evolution by spreading of the sea floor. *Nature*, 1961, **190**, 854–857.
3. Hess, H. H., History of ocean basins. *Petrologic Studies*, A volume to honor A. F. Buddington (eds Engel, A. E. J., James, H. L. and Leonard, B. F.), Geol. Soc. Am., New York, 1962, pp. 599–620.
4. Vine, F. J. and Matthews, D. H., Magnetic anomalies over oceanic ridges. *Nature*, 1963, **199**, 947–949.
5. Basaltic Volcanism Study Project, Pergamon Press, New York, 1981, p. 1286.
6. Engel, C. G., Fisher, R. L. and Engel, A. E. J., Igneous rocks of the Indian Ocean floor. *Science*, 1965, **150**, 605–610.
7. Raitt, R., The crustal rocks. *The Sea* (ed. Hill, M. N.), John Wiley, New York, 1963, vol. 3, pp. 85–102.
8. Schilling, J. G., Unni, C. K. and Bender, M. L., Origin of chlorine and bromine in the oceans. *Nature*, 1978, **273**, 631–636.
9. Crisp, J. A., Rates of magma emplacement and volcanic output. *J. Volcanol., Geotherm. Res.*, 1984, **20**, 177–211.
10. Lisitzin, A. P., Oceanic sedimentation lithology and geochemistry. Am. Geophys. Union, Washington DC, 1996, p. 400.
11. Schlich, R., *The Indian Ocean: Aseismic Ridges, Sprean Basins and Margins* (eds Nairn, A. E. M. and Stehli, F. G.), Plenum Press, New York, 1982, pp. 51–147.
12. Heezen, B. C. and Tharp, M., Physiographic diagram of the Indian Ocean (with descriptive sheet). Geol. Soc. Am., New York, 1965.
13. Udintsev, G. B. (ed.) *Geological-Geophysical Atlas of the Indian Ocean*, Pergamon Press, Oxford, 1975, p. 151.
14. Haxby, W. F., Gravity field of world's oceans (color map), Lamont Doherty Geological Observatory of Columbia Univ., Palisades, New York, 1985.
15. Perfit, M. R. and Chadwick, Jr. W. W., Magmatism at mid-ocean ridge: Constraints from volcanological and geochemical investigations. *Faulting and Magmatism* (eds Buck, W. R., Delaney, P. T., Karson, J. R. and Lagabriele, Y.), Geophys. Monogr., Am. Geophys. Union, Washington DC, 1998, pp. 59–115.
16. McBirney, A. R., Oceanic volcanism: a review. *Rev. Geophys. Space Phys.*, 1971, **9**, 523–556.
17. Purdy, G. M., Kong, L. S. L., Christeson, G. L. and Solomon, S. C., Relationship between spreading rate and the seismic structure of mid-ocean ridges. *Nature*, 1992, **355**, 815–817.
18. Phipps-Morgan, J. and Chen, Y. J., Dependence of ridge-axis morphology on magma supply and spreading rate. *Nature*, 1993, **364**, 706–708.
19. Klein, E. and Langmuir, C. H., Global correlations of ocean ridge basaltic chemistry with axial depth and crustal thickness. *J. Geophys. Res.*, 1987, **92**, 8089–8115.
20. Niu, Y. and Batiza, R., An empirical method for calculating melt compositions produced beneath mid-ocean ridges: Application for axis and off-axis seamounts melting. *J. Geophys. Res.*, 1993, **96**, 21,753–21,777.
21. Hall, M., Note upon a portion of basalt from Mid-Atlantic. *Min. Mag.*, 1876, **1**, 1–3.
22. Kay, R., Hubbard, N. J. and Gast, P. W., Chemical characteristics and origin of oceanic ridge volcanic rocks. *J. Geophys. Res.*, 1970, **75**, 1585–1613.
23. Bryan, W. B., Thompson, G., Frey, F. A. and Dickey, Jr. J. S., Inferred geological settings and differentiation in basalts from the Deep Sea Drilling Project. *J. Geophys. Res.*, 1976, **81**, 4285–4304.
24. Condie, K. C., *Plate Tectonics and Crustal Evolution*, Pergamon Press, New York, p. 318.
25. Mislankar, P. G. and Iyer, S. D., Petrographical indicators of petrogenesis: examples from Central Indian Ocean Basin basalts. *Ind. J. Mar. Sci.*, 2001, **30**, 1–8.
26. Wilson, M., *Igneous Petrogenesis*, Kluwer Acad. Publ., Dordrecht, 2000, p. 466.
27. Flower, M. F. J., Accumulation of calcic plagioclase in ocean-ridge tholeiite: an indicator of spreading rate. *Nature*, 1980, **287**, 530–532.
28. Miyashiro, A., Shido, F. and Ewing, M., Crystallization and differentiation in abyssal tholeiites and gabbros from mid-oceanic ridges. *Earth Planet. Sci. Lett.*, 1970, **7**, 361–365.
29. Bougault, H. and Hekinian, R., Rift valley in the Atlantic Ocean near 36°50'N: petrology and geochemistry of basaltic rocks. *Earth Planet. Sci. Lett.*, 1974, **24**, 249–261.
30. Blanchard, D. P., Rhodes, J. M., Dungan, M. S., Rodgers, K. V., Donaldson, C. H., Brannon, J. C., Jacobs, J. W. and Gibson, E. K., The chemistry and petrology of basalts from Leg 37 of the Deep Sea Drilling Project. *J. Geophys. Res.*, 1976, **81**, 4231–4247.
31. Cann, J. R., Basalts from the ocean floor. *The Sea* (ed. Emiliani, C.), John Wiley, New York, 1981, vol. 7, pp. 363–390.
32. Schilling, J. G., Zajhara, M., Evans, R., Johnson, T., White, W., Devine, J. D. and Kingsley, R., Petrologic and geochemical variations along the Mid-Atlantic Ridge from 29°N to 73°N. *Am. J. Sci.*, 1983, **283**, 510–586.
33. Vogt, P. R., Plumes, subaxial pipe flow and topography along the mid-ocean ridge. *Earth Planet. Sci. Lett.*, 1976, **29**, 309–325.
34. Le Roex, A. P., Dick, H. J. B. and Watkins, R. T., Petrogenesis of anomalous K-enriched MORB from the Southwest Indian Ridge: 11°53'E to 14°38'E. *Contrib. Mineral. Petrol.*, 1992, **110**, 253–268.
35. Reynolds, J. A., Langmuir, C. H., Bender, J. F., Kastens, K. A. and Bryan, W. B. F., Spatial and temporal variability in the geochemistry of basalts from the East Pacific Rise. *Nature*, 1992, **359**, 493–499.
36. Michael, P. J. and Cornell, W. C., Influence of spreading rate and magma supply on crystallization at mid-ocean ridges: evidence from chlorine and major element chemistry. *J. Geophys. Res.*, 1998, **103**, 18,325–18,356.
37. Sinton, J. M. and Detrick, R. S., Mid-ocean ridge magma chambers. *J. Geophys. Res.*, 1992, **97**, 197–216.
38. Grove, T. L., Kinzler, R. J. and Bryan, W. B., Fractionation of mid-ocean ridge basalts. *Mantle Flow and Melt Generation at Mid-Ocean Ridges* (eds Phipps-Morgan, J., Blackman, D. K. and Sinton, J.), Geophys. Monogr., Am. Geophys. Union, Washington, DC, 1992, pp. 281–310.
39. Langmuir, C. H., Klein, E. and Plank, T., Petrological systematics of mid-ocean ridge basalts: constraints on melt generation beneath ocean ridges. *Mantle Flow and Melt Generation at Mid-Ocean Ridges* (eds Phipps-Morgan, J., Blackman, D. K. and Sinton, J. M.), Am. Geophys. Union, Washington, DC, 1992, 71, pp. 183–280.
40. Hofmann, A. W., Mantle geochemistry: the message from oceanic volcanism. *Nature*, 1997, **385**, 219–229.
41. O'Hara, M. J., Geochemical evolution during fractional crystallization of a periodically refilled magma chamber. *Nature*, 1977, **266**, 503–507.
42. Banerjee, R. and Iyer, S. D., Petrography and chemistry of basalts from the Carlsberg Ridge. *J. Geol. Soc. India*, 1991, **38**, 369–386.

43. Iyer, S. D. and Banerjee, R., Mineral chemistry of Carlsberg Ridge basalts at 3°35'–3°41' N. *Geo-Mar. Lett.*, 1993, **13**, 153–158.
44. Schilling, J. G., After mantle plume: rare earth evidence. *Nature*, 1973, **242**, 2–5.
45. Subbarao, K. V. and Hekinian, R., Alkali-enriched rocks from the Central-Eastern Pacific Ocean. *Mar. Geol.*, 1978, **26**, 249–268.
46. Dupre, B. and Allegre, C. J., Pb–Sr isotope variation in Indian Ocean basalts and mixing phenomenon. *Nature*, 1983, **303**, 142–146.
47. Hamelin, B. and Allegre, C. J., Large scale regional units in the depleted upper mantle revealed by an isotope study of the South West Indian Ridge. *Nature*, 1985, **315**, 196–199.
48. Macdonald, K. C., Mid Ocean Ridges: fine scale tectonic, volcanic, and hydrothermal processes within the plate boundary. *Ann. Rev. Earth Planet. Sci.*, 1982, **10**, 155–190.
49. Hart, S. R., Mantle domains: signatures, genesis and mixing chronologies. *Nature*, 1988, **90**, 273–276.
50. O'Hara, M. J. and Mathews, R. E., Geochemical evolution in an advancing, periodically-tapped, continuously refilled magma chamber. *J. Geol. Soc. Lond.*, 1981, **138**, 237–277.
51. Rosendahl, B. R., Raitt, R. W., Dorman, L. M., Bibee, L. D., Hussong, D. M. and Sutton, G. H., Evolution of oceanic crust. 1: A physical model of the East Pacific Rise crest derived from seismic refraction data. *J. Geophys. Res.*, 1976, **81**, 5294–5304.
52. Kuznir, N. J., Thermal evolution of the oceanic crust: its dependency on spreading rate and effect on crustal structure. *Geophys. J. R. Astron. Soc.*, 1980, **61**, 167–181.
53. Toomey, D. R., Solomon, S. C. and Purdy, G. M., Microearthquakes beneath the median valley of the Mid-Atlantic Ridge near 23°N: tomography and tectonics. *J. Geophys. Res.*, 1988, **93**, 9093–9112.
54. Purdy, G. M. and Detrick, R. S., Crustal structure of the Mid-Atlantic Ridge at 23°N from seismic refraction studies. *J. Geophys. Res.*, 1986, **91**, 3739–3762.
55. Nisbet, E. G. and Fowler, C. M. R., The Mid-Atlantic Ridge at 37 and 45°N: some geophysical and petrological constraints. *Geophys. J. R. Astron. Soc.*, 1978, **54**, 631–660.
56. Langmuir, C. H., Bender, J. F. and Batiza, R., Petrology and tectonic segmentations of the Eastern Pacific Rise: 5°30'–14°30'E. *Nature*, 1986, **322**, 422–429.
57. Kushiro, I., Partial melting experiments on peridotite and origin of mid-ocean ridge basalt. *Annu. Rev. Earth Planet. Sci.*, 2001, **29**, 71–107.
58. Batiza, R., Magmatic segmentation of mid-ocean ridges: a review. *Tectonic, Magmatic, Hydrothermal and Biological Segmentation of Mid-Ocean Ridges* (eds Macleod, C. J., Tyler, P. A. and Walker, C. L.), Geol. Soc. Spl. Publ., London, 1996, vol. 118, pp. 103–130.
59. Kinzler, R. J., Magmatism at ocean ridges. *Rev. Geophys. Suppl.*, 1995, 63–69.
60. Iyer, S. D., Alteration of basaltic glasses from the Central Indian Ocean. *J. Geol. Soc. India*, 1999, **54**, 609–620.
61. Hart, S. R., K, Rb, Cs contents and K/Rb, K/Cs altered submarine basalts. *Earth Planet. Sci. Lett.*, 1969, **6**, 295–303.
62. Natland, J. H., Mineralogy and crystallization of oceanic basalts. *Oceanic Basalts* (ed. Floyd, P. A.), Blackie & Sons, Glasgow, 1991, pp. 63–93.
63. Hart, R. A., Chemical exchange between seawater and deep ocean basalts. *Earth Planet. Sci. Lett.*, 1970, **9**, 269–279.
64. Fisher, R. L., Sclater, J. G. and McKenzie, D. P., Evolution of the Central Indian Ridge, Western Indian Ocean. *Bull. Geol. Soc. Am.*, 1971, **82**, 553–562.
65. Engel, C. G. and Fisher, R. L., Granitic to ultramafic rock complexes of the Indian Ocean ridge system, Western Indian Ocean. *Bull. Geol. Soc. Am.*, 1975, **86**, 1553–1578.
66. DeMets, C., Gordon, R. G. and Vogt, P., Location of the Africa–Australia–India triple junction and motion between the Australian and Indian plates: results from an aeromagnetic investigation of the central Indian and Carlsberg ridges. *Geophys. J. Int.*, 1994, **119**, 893–930.
67. Royer, J.-Y., Gordon, R. G., DeMets, C. and Vogt, P. R., New limits on the motion between India and Australia since chron 5 (11 Ma) and implications for lithospheric deformation in the equatorial Indian Ocean. *Geophys. J. Int.*, 1997, **129**, 41–74.
68. Parsons, L. M., Patriat, P., Searle, R. C. and Briais, A. R., Segmentation of the Central Indian Ridge between 12°12'S and the Indian Ocean Triple Junction. *Mar. Geophys. Res.*, 1993, **15**, 265–282.
69. Price, R. C., Kennedy, A. K., Riggs-Sneeringer, M. and Frey, F. A., Geochemistry of basalts from the Indian Ocean triple junction: implications for the generation and evolution of Indian Ocean ridge basalts. *Earth Planet. Sci. Lett.*, 1986, **78**, 379–396.
70. Drolia, R. K., Ghose, I., Subramanyam, A. S., Malleswara Rao, M. M., Kessarkar, P. and Murthy, K. S. R., Magnetic and bathymetric investigations over the Vema region of the Central Indian Ridge: Tectonic implications. *Mar. Geol.*, 2000, **167**, 413–423.
71. Chaubey, A. K., Krishna, K. S., Subba Raju, L. V. and Gopala Rao, D., Magnetic anomalies across the southern Central Indian Ridge: Fault. *Deep-Sea Res.*, 1990, **37**, 647–656.
72. Kamesh Raju, K. A., Ramprasad, T. and Subrahmanyam, C., Geophysical investigations over a segment of the Central Indian Ridge, Indian Ocean. *Geo-Mar. Lett.*, 1997, **17**, 195–201.
73. Radha Krishna, M., Seismic moment release along selected major transforms on the Central Indian Ridge, Western Indian Ocean and its tectonic implications. *Proc. Indian Acad. Sci. (Earth Planet. Sci.)*, 1995, **104**, 693–706.
74. Royer, J.-Y., Sclater, J. G. and Sandwell, S. T., A preliminary tectonic fabric chart of the Indian Ocean. *Proc. Indian Acad. Sci. (Earth Planet. Sci.)*, 1989, **98**, 7–24.
75. Farquharson, W. I., Topography. *Sci. Rept. John Murray Exped.*, (1933–34), 1935, vol. 1, pp. 43–61.
76. Backman, J. et al., *Proc. ODP Init. Repts. College Station, TX (Ocean Drilling Program)*, 1988, p. 115.
77. Mukhopadhyay, R. and Iyer, S. D., Petrology of tectonically segmented Central Indian Ridge. *Curr. Sci.*, 1993, **65**, 623–628.
78. Kalyayev, G. I., Karabovich, S. V., Rusakov, O. M. and Starostenkov, V. I., Deep structure of the Arabian-Indian Ridge and the Owen fault zone. *Geotect.*, 1983, **17**, 32–42.
79. Subbarao, K. V., Kempe, D. R. C., Reddy, V. V., Reddy, G. R. and Hekinian, R., Review of the geochemistry of Indian and other oceanic rocks. *Origin and Distribution of the Elements* (ed. Ahrens, L. H.), Pergamon Press, Oxford, 1979, pp. 367–399.
80. Frey, F. A., Dickey, J. S. Jr., Thompson, G., Bryan W. B. and Davies, H. L., Evidence for heterogeneous primary MORB and mantle sources, NW Indian Ocean. *Contrib. Mineral. Petrol.*, 1980, **74**, 387–402.
81. Dosso, L., Bougault, H., Beuzart, P., Calvez, J. Y. and Joron, J. L., The geochemical structure of the Southeast Indian Ridge. *Earth Planet. Sci. Lett.*, 1988, **88**, 47–59.
82. Subbarao, K. V. and Hedge, C. E., K, Rb, Sr, and ⁸⁷Sr/⁸⁶Sr in rocks from the Mid-Indian Oceanic Ridge. *Earth Planet. Sci. Lett.*, 1973, **18**, 223–228.
83. Subbarao, K. V., Reddy, V. V., Hekinian, R. and Chandrasekharan, D., Large ion lithophile elements and Sr and Pb isotopic variation in the Indian Ocean. *Indian Ocean Geology and Biostratigraphy* (eds Heirtzler, J. R., Bolli, H. M., Davies, T. A., Saunders, J. B. and Sclater, J. G.), Am. Geophys. Union, Lithocrafters, Washington, DC, 1977, pp. 259–278.
84. Reddy, V. V., Subbarao, K. V., Reddy, G. R., Matsuda, J. and Hekinian, R., Geochemistry of volcanics from the Ninetyeast Ridge and its vicinity in the Indian Ocean. *Mar. Geol.*, 1978, **26**, 99–117.
85. Herzig, P. M. and Pluger, W. L., Exploration for hydrothermal activity near the Rodriguez Triple Junction, Indian Ocean. *Cand. Min.*, 1988, **26**, 721–736.

86. Rehkamper, M. and Hofmann, A. W., Recycled ocean crust and sediment in Indian Ocean MORB. *Earth Planet. Sci. Lett.*, 1997, **147**, 93–106.
87. Mudholkar, A. V., Magmatic evolution of the fresh basalts from the ridge axis near Egaria fracture zone, Central Indian Ridge. *J. Geol. Soc. India*, 2001, **58**, 329–339.
88. Hekinian, R., Gabbro and pyroxenite from a deep-sea core in the Indian Ocean. *Mar. Geol.*, 1970, **9**, 287–294.
89. Fisher, R. L., Dick, H. J. B., Natland, J. H. and Meyers, P. S., Mafic/ultramafic suites of the slowly spreading Southwest Indian Ridge: Protea exploration of the Antarctic plate boundary, 24°E–47°E. *Ophioliti*, 1986, **11**, 147–178.
90. Bloomer, S. H., Natland, J. H. and Fisher, R. L., Mineral relationships in gabbroic rocks from fracture zones of Indian Ocean ridges: evidence for extensive fractionation, parental diversity and boundary-layer recrystallization. *Magmatism in the Ocean Basin* (eds Saunders, A. D. and Norry, M. J.), Spl. Publ., #42 Geol. Soc., Oxford, 1989, pp.107–124.
91. Ito, E., White, W. M. and Göpel, C., The O, Sr, Nd, and Pb isotope geochemistry of MORB. *Chem. Geol.*, 1987, **62**, 157–176.
92. Hedge, C. E., Watkins, N. D., Hildreth, R. A. and Doering, W. P., ⁸⁷Sr/⁸⁶Sr ratios in basalts from islands in the Indian Ocean. *Earth Planet. Sci. Lett.*, 1973, **21**, 29–34.
93. Mahoney, J. J., le Roex, A. P., Peng, Z., Fisher, R. L. and Natland, J. H., Western limits of Indian MORB mantle and the origin of low ²⁰⁶Pb/²⁰⁴Pb MORB isotope systematics of the central Southwest Indian Ridge (17–50°E). *J. Geophys. Res.*, 1992, **97**, 19,771–19,790.
94. Weis, D. and Frey, F. A., Role of Kerguelen plume in generating the eastern Indian Ocean seafloor. *J. Geophys. Res.*, 1996, **101**, 13,831–13,849.
95. Nishio, Y., Ishii, T., Gamo, T. and Sano, Y., Volatile element isotopic systematics of the Rodriguez Triple Junction Indian Ocean MORB: implications for mantle heterogeneity. *Earth Planet. Sci. Lett.*, 1999, **170**, 241–253.
96. Ghatak, S. K., Babu, C. C. and Ghose, N., Magnetic lineations in the Indian Ocean around Carlsberg Ridge, *Geol. Surv. India Mar. Wing Newslett.*, 1995, **11**, 8–9.
97. Bhattacharjee, D., Micropaleontological evidences of possible hydrothermal activities in the Carlsberg Ridge, Indian Ocean. *Geol. Surv. India Mar. Wing Newslett.*, 1997, **13**, 6–7.
98. Mukhopadhyay, R., Murthy, K. S. R., Iyer, S. D., Malleswara Rao, M. M., Banerjee, R., Subramanyam, A. S., Shirodkar, P. V. and Ghose, I., InRidge program: Preliminary results from the first cruise. *Curr. Sci.*, 1998, **75**, 1157–1161.
99. Mukhopadhyay, R., Iyer, S. D., Banerjee, R. and Droliia, R. K., Studying the Indian Ocean Ridge System: Agenda for the new century. *J. Geol. Soc. India*, 1999, **54**, 659–661.
100. Droliia, R. K., Mukhopadhyay, R. and Iyer, S. D., Carlsberg-Central Indian Ridge: a case for InterRidge working group. *InterRidge News*, 2000, **9**, 12–13.
101. Mudholkar, A.V., Kodagali, V. N., Kamesh Raju, K. A., Valsangkar, A. B., Ranade, G. H. and Ambre, N. V., Geomorphological and petrological observations along a segment of slow-spreading Carlsberg Ridge. *Curr. Sci.*, 2002, **82**, 982–989.
102. Ashalatha, B. and Singh, R. N., Effects of fluid circulation on the thermal structure of evolving lithosphere: application to Carlsberg Ridge. *J. Geol. Soc. India*, 2001, **58**, 351–359.
103. Rao, P. S., Kamesh Raju, K. A., Ramprasad, T., Nath, B. N., Rao, B. R., Rao, M. Ch. and Nair, R. R., Evidence for hydrothermal activity in the Andaman Backarc Basin. *Curr. Sci.*, 1996, **70**, 379–385.
104. Chernova, T. G., Rao, P. S., Pikovskii, Alekseeva, T. A., Nath, B. N., Rao, B., R. and Rao, The composition and the source of hydrocarbons in sediments taken from the tectonically active Andaman Backarc Basin, Indian Ocean. *Mar. Chem.*, 2001, **75**, 1–15.
105. Melson, W. G., Vallier, T. L., Wright, T. L., Byerly, G. and Nelen, J., Chemical diversity of abyssal volcanic glass erupted along Pacific, Atlantic and Indian Ocean seafloor spreading centers. *The Geophysics of the Pacific Ocean Basin and its Margin* (eds Sutton, G. H., Manghnani, M. and Moberly, R.), Am. Geophys. Union, Washington DC, 1976, pp. 351–367.
106. Sun, S.-S., Nesbitt, R. W. and Sharaskin, A. Y., Geochemical characteristics of mid-ocean ridge basalts. *Earth Planet. Sci. Lett.*, 1979, **44**, 119–138.
107. Cohen, R. S., Everson, N. M., Hamelin, P. J. and Onions R. K., U–Pb, Sm–Nd and Rb–Sr systematics of mid-ocean ridge basalt glasses. *Nature*, 1980, **283**, 149–154.
108. Mahoney, J. J., Natland, J. H., White, W. M., Poreda, R., Blommer, S. H., Fisher, R. L. and Baxter, A. N., Isotopic and geochemical provinces of the western Indian Ocean spreading center. *J. Geophys. Res.*, 1989, **94**, 4033–4052.
109. Hamelin, B., Dupre, B. and Allegre, C.J., Lead-strontium isotopic variation along the East Pacific Rise and the Mid-Atlantic Ridge. *Earth Planet. Sci. Lett.*, 1984, **67**, 340–350.
110. Batiza, R., Petrology and geochemistry of eastern Pacific spreading centers. *The Eastern Pacific Ocean and Hawaii: The Geology of North America* (eds Winterer, E. L., Hussong, D. M. and Decker, R. W.), Geol. Soc. Am., Boulder, Colorado, 1989, pp. 145–160.
111. ETOPO5 Relief map of the Earth's surface, AGU. *EOS Trans.*, 1986, **67**, 121.

ACKNOWLEDGEMENTS. We acknowledge the Director for encouraging the on-going InRidge project and the Office of the Naval Research, USA for extending financial support. We thank Prof. K. V. Subbarao and Dr S. M. Karisiddaiah for their reviews that helped improve the quality of the paper and Drs M. Shyam Prasad and R. Mukhopadhyay for suggestions. A. Y. Mahale assisted in preparing the figures. NIO's contribution # 3830.